CFD MODELLING OF CHUGGING CONDENSATION REGIME OF BWR SUPPRESSION POOL EXPERIMENTS

V. Tanskanen*, G. Patel, M. Puustinen, E. Hujala, R. Kyrki-Rajamäki and J. Hyvärinen
LUT School of Energy Systems/Nuclear Engineering
Lappeenranta University of Technology (LUT), PO Box 20, FIN-53851 Lappeenranta, Finland
vesa.tanskanen@lut.fi; giteshkumar.patel@lut.fi; markku.puustinen@lut.fi; rkyrki@lut.fi;
juhani.hyvarinen@lut.fi

ABSTRACT

In this work, the chugging direct contact condensation (DCC) mode of BWR suppression pool operation is simulated by using Eulerian-Eulerian two-fluid approach of the compressible flow NEPTUNE_CFD software and the OpenFOAM CFD code. The interfacial heat transfer between steam and water is modeled by using condensation models based on the surface renewal theory. Flow turbulence is solved by employing the standard k-ε turbulence model. As the condensation rate could not be measured experimentally, a pattern recognition algorithm was used to extract information about the bubble size and the chugging frequency during the steam discharges. The experimental references for the analysis and simulations have been obtained from the suppression pool test facility experiments of the Lappeenranta University of Technology. The reference cases contain steam discharges within the open pool test facility POOLEX and within the pressurizing drywell-wetwell test facility PPOOLEX. The simulation results indicate that the qualitative nature of chugging can be captured well with the computational fluid dynamics (CFD) modelling and better quantitative results can be reached by DCC model development.

KEYWORDS
Suppression pool, Chugging, Pattern recognition, CFD, Direct contact condensation

1. INTRODUCTION

In the most current boiling water reactors (BWR), the containment has been designed to be a compact structure, relying on pressure suppression to mitigate overpressurization in case of operational transients and postulated loss of coolant accidents (LOCAs). Pressure suppression in the containment is achieved by a condensation pool, a sub-cooled water pool into which steam is vented [1]. The condensation rate has to be high for the suppression pool system to fulfill its safety function. Depending on discharge conditions, different direct contact condensation (DCC) modes may arise, making condensation modelling challenging both in experiments and in numerical simulations. As to the experiments, the condensation induced pressure oscillations are often unfavorably violent for the delicate measurement instrumentation.

Regarding the numerical simulations, the pressure oscillations are challenging for most of the incompressible flow solvers of the CFD softwares. Oscillatory condensation modes, including chugging, have been modelled analytically in a few studies e.g. in [2] and [3]. Analytical and empirical findings have recently been applied to CFD-like lumped parameter code GOTHIC in order to simulate stratification and mixing phenomena in suppression pools in a numerically economic way [4]. Pure CFD simulations of chugging DCC in vertical vent pipes are rare. Volume of Fluid (VOF) simulations without mass transfer have been presented [5-6] and some VOF simulations with mass transfer have been attempted [7]. More

* Corresponding author

recently, Eulerian simulation results with heat and mass transfer have been presented [8-10]. Otherwise many of the recent suppression pool CFD simulations have been made with nozzle or sparger systems, e.g. [11-12]. The authors of [9] and [13] presented preliminary results of the improved capability of Eulerian two-phase CFD codes to successfully model and predict chugging DCC in a POOLEX suppression pool test of Lappeenranta University of Technology (LUT). They introduced a pattern recognition approach where condensation rate can be analyzed indirectly from the video material of the suppression pool tests. They simulated example cases of chugging at subcooling levels of 30K, 40K and 60K in the open-top pool system POOLEX [13]. These simulations used the Hughes and Duffey heat transfer correlation [14] and resulted in qualitatively realistic chugging behavior. The main results of those simulations are summarized in this paper as well. This paper presents the first NEPTUNE_CFD results and findings from the simulations of the drywell-wetwell suppression pool system PPOOLEX of LUT. Preliminary results of the OpenFOAM simulations of an open-top pool case are compared with the earlier NEPTUNE_CFD results as well.

2. POOLEX AND PPOOLEX EXPERIMENTS

2.1. The STB-28 and DCC-05 tests

The first test facility constructed for BWR containment studies at LUT was called POOLEX [15]. It was a cylindrical pool with an open top and a conical bottom part, and it modelled the wetwell of a suppression pool. The inner diameter of the pool was 2.4 m and the height 5.0 m. A vertical DN200 blowdown pipe was placed inside the pool in a non-axisymmetric location, i.e. 300 mm from the pool center. The pool was filled with water to the level of 3.5 m in the test set-ups, which left the blowdown pipe submerged by 2 m.

The later PPOOLEX facility modeling BWR containment includes a wetwell compartment (suppression pool), drywell compartment, inlet plenum and air/steam line piping. The main component of the facility is the approximately 31 m^3 cylindrical test vessel, 7.45 m in height and 2.4 m in diameter. The facility is able to withstand overpressure up to 4 bar and underpressure of 0.5 bar. Windows on the side walls and in the bottom segment of the test vessel allow visual observation of the phenomena during the tests. The drywell compartment is thermally insulated. A DN100 blowdown pipe was used in the later PPOOLEX experiments (including the DCC-05 test discussed in this paper) and it was positioned inside the pool in a non-axisymmetric location, i.e. 420 mm away from the centerline of the pool. The steam generators of the PACTEL facility [16] were used as a steam source during the tests with both of the facilities (Fig. 1).

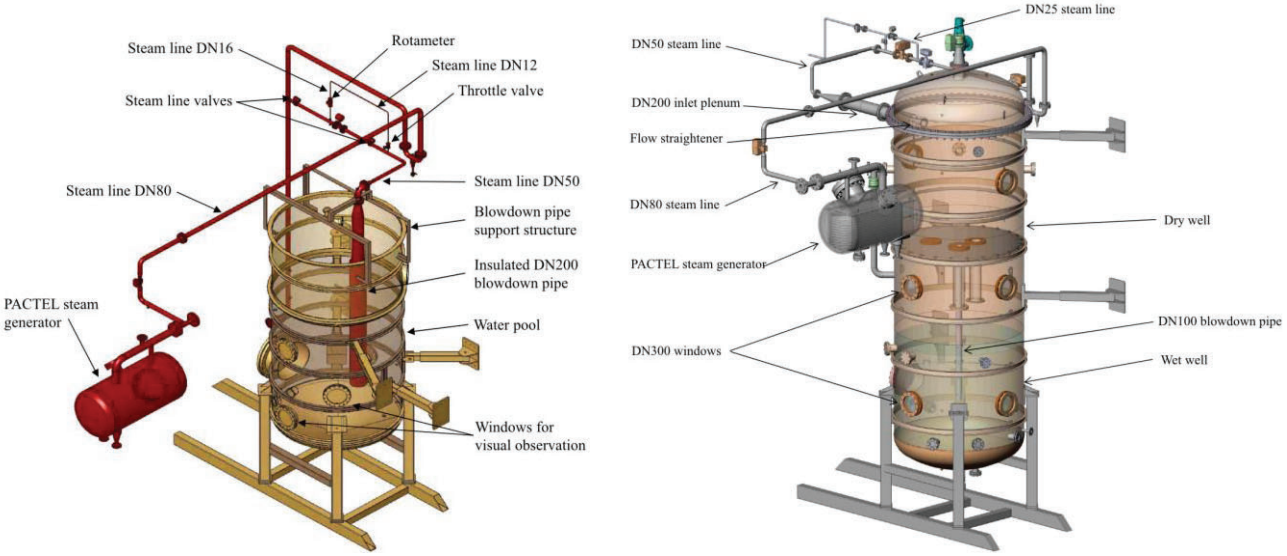

Figure 1. POOLEX and PPOOLEX test facilities [15].

The POOLEX STB-28 experiment consisted of one long-running steam blowdown (duration 3195 s). The purpose of this test was to study the formation and condensation of steam bubbles at the blowdown pipe outlet as a function of pool water temperature. During the blowdown, seven short periods (duration 12 . . . 30 s) were recorded with a higher sampling rate and labelled from STB-28-1 to STB-28-7. The pool water temperature rose from 47 °C to 77 °C during the test. The steam mass flow rate was kept at the level of 0.3 kg/s for the whole blowdown. Fig. 2 shows the measured values of inlet mass flow rate, steam temperature and pool temperature and the estimated values of condensation rates and pipe wall temperature during the STB-28 test.

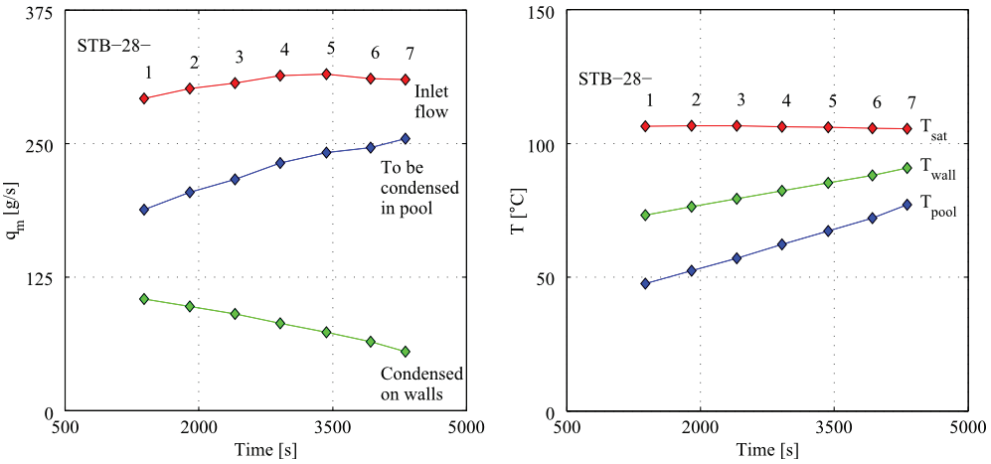

Figure 2. Estimation of wall condensation rate and wall temperatures in the STB-28 test.

Condensation on the wall of the submerged blowdown pipe was estimated by using the correlation of Chen et al. [17, 18 and 9]. During the blowdown, chugging was the dominating condensation mode. For this reason, steam bubbles of different sizes formed and collapsed at the blowdown pipe outlet. The bubbles were small in the early phase of the test. As the pool water temperature rose, dominating bubble size increased gradually as well. Fig. 3 shows some typical steam bubbles that formed during the STB-28 experiment. The test facility instrumentation in the STB-28 test contained a high speed camera (500 fps), a standard speed camera (25 fps), various thermocouples and pressure transducers within the pool and blowdown pipe and stress strain sensors on the pool bottom.

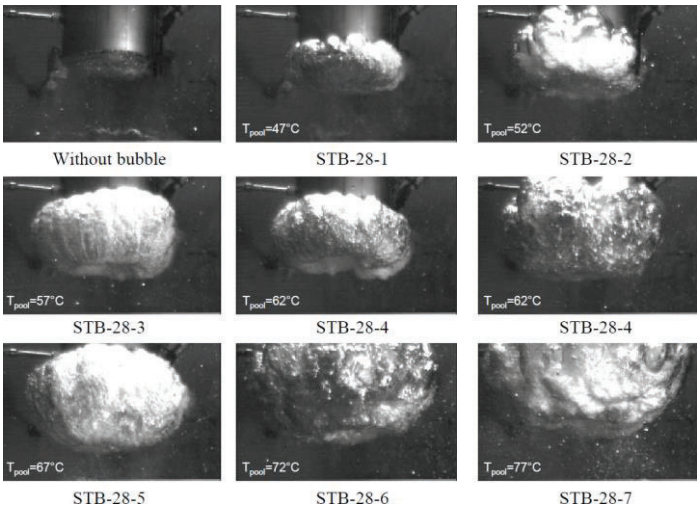

Figure 3. Maximally expanded bubbles as a function of pool water temperature in the STB-28 test.

The main purpose of the PPOOLEX DCC-05 experiment was to obtain data for the validation of the DCC models used in CFD codes and to make 3D high speed video recordings to be used in the development work of the pattern recognition algorithms. In order to get long enough camera samples, the resolution of the cameras was set to 768x768 px and the framerate to 300 fps. These settings allowed capturing 6 pieces of 48 second samples from each test part.

Before the DCC-05 experiment the wetwell pool was filled with almost isothermal water (25 °C) so that the blowdown pipe outlet was submerged by ~1.0 m. The drywell compartment of the test vessel was full of air at atmospheric pressure. During the clearing phase, part of the steam condensed on the drywell walls until the structures had heated up. Practically all air was displaced from the drywell into the gas space of the wetwell after 500 seconds of the experiment start. After that, the idea was to keep the pool water temperature as constant as possible but use a large range of different steam flow rates. To achieve this goal the steam flow rate was quickly adjusted to the new value for the recorded periods, but during data transferring periods it was reduced to almost zero to prevent the unnecessary heat-up of pool water. Regardless of that, the temperature of pool water at the blowdown pipe outlet elevation rose about 10 K during the investigated period. Steam flow rates between 75 and 200 g/s were used in the chugging blows of DCC-05 (Fig. 4).

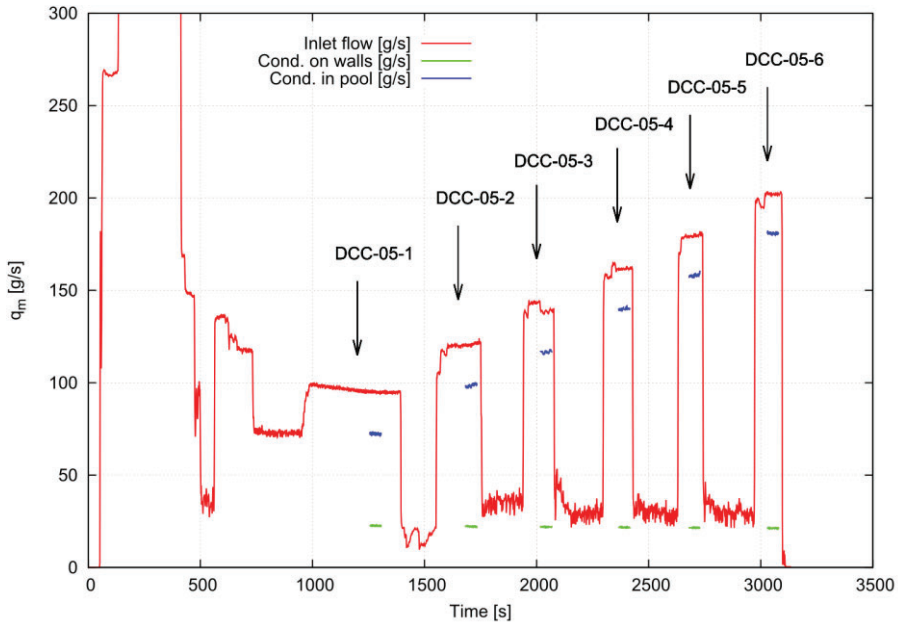

Figure 4. Six chugging blows of the DCC-05 experiment.

Fig. 5 shows an example of a collapsing bubble in the test. Recognized bubble boundaries of the pattern recognition algorithm are marked on red. The individual steam blows of the DCC-05 experiment defined by the steam mass flux and pool bulk temperature are marked on the condensation mode map of Lahey and Moody [1] in Fig. 6.

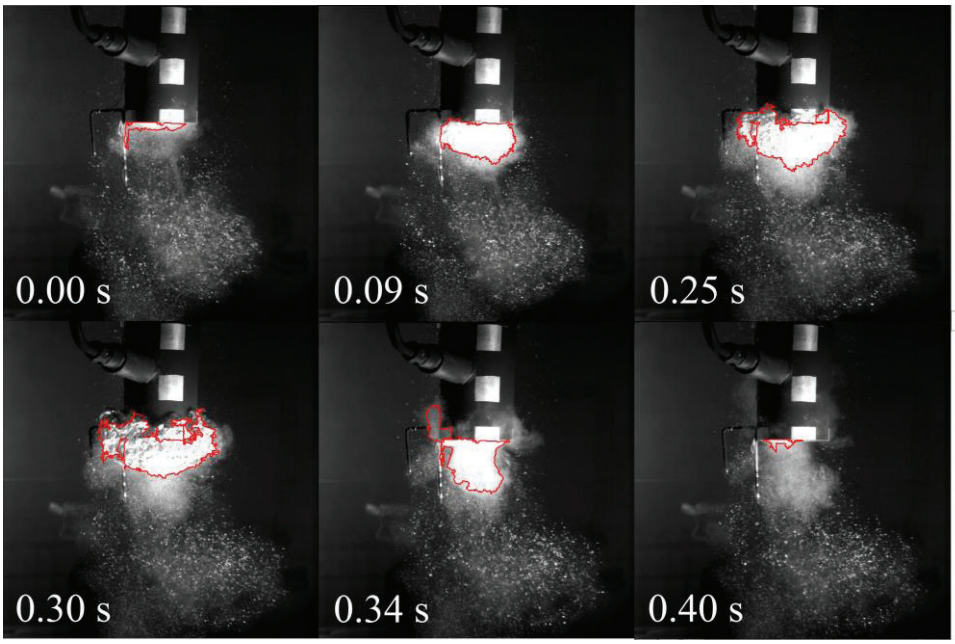

Figure 5. Expansion and collapse of a bubble during the later phase of the DCC-05-4 test. The boundaries recognized by the pattern recognition algorithm marked as red.

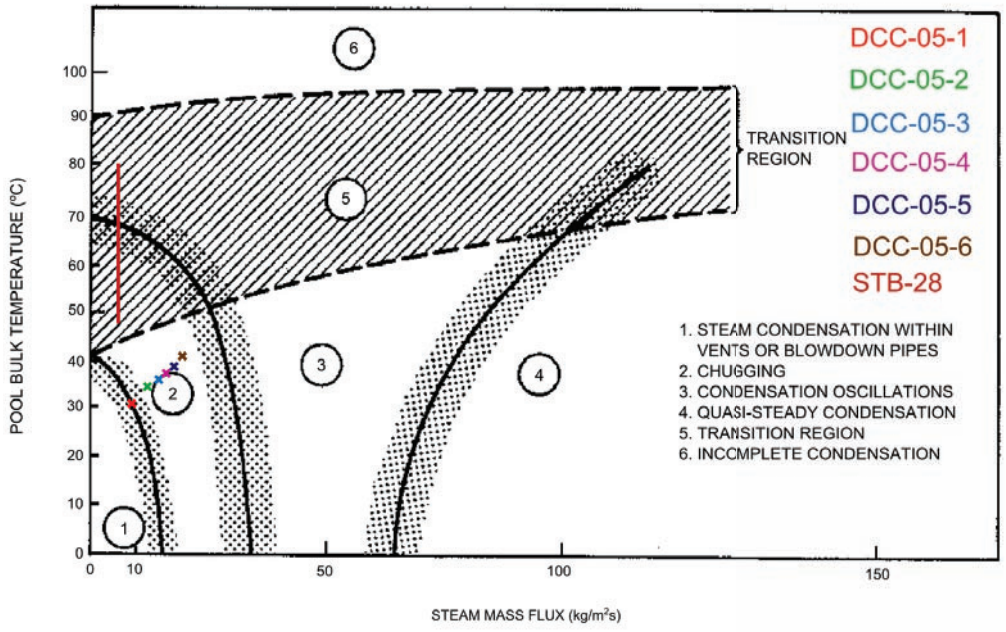

Figure 6. Steam blows of the STB-28 and DCC-05 tests on the condensation mode map [1].

2.2. Pattern Recognition

A pattern recognition algorithm for evaluation of bubble mean diameters was created tailored for the STB-28 high speed camera data [9]. The algorithm was based on a single camera output. For the DCC-05 experiments, the algorithm was upgraded to use three almost perpendicularly located high speed cameras. Fig. 5 shows a recognized bubble boundaries of the left side camera (marked in red). The 3D view obtainable by using all the cameras should improve the accuracy of evaluation of the bubble volume, the surface area, and also the Sauter mean diameter. The chugging frequencies were evaluated also by using

the pattern recognition algorithm. Fig. 7 shows cross-sectional areas of the bubbles of the side cameras compared to the pressure measurements p_5 below the pipe's outlet and pressure p_6, at the bottom of the pool. It can be clearly seen that the biggest pressure changes will appear immediately after the biggest bubbles.

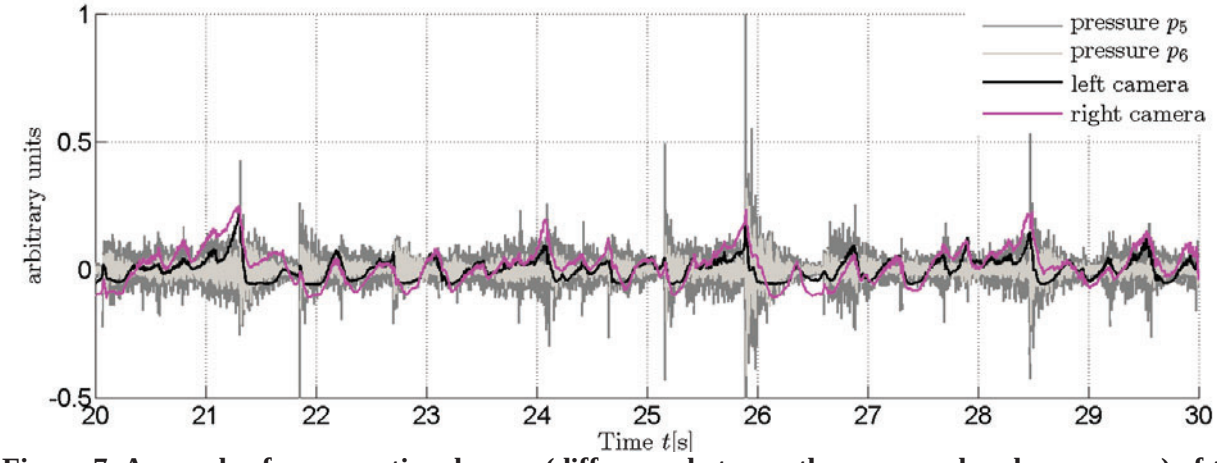

Figure 7. A sample of cross-sectional areas (difference between the measured and mean area) of the bubbles compared to the pressure p_5 outside the pipe's outlet and pressure p_6 at the bottom of the pool in arbitrary units in the DCC-05-4 experiment.

3. MODELING AND SIMULATION STRATEGIES

3.1. Physical Models

The chugging phenomenon in vertical blowdown pipe causes strong pressure oscillations due to the extensive and rapid phase change. Compressible flow formulation is hence preferable for simulation of such conditions. The compressible flow Eulerian Finite Volume multi-field solver NEPTUNE_CFD [19-21] versions 1.0.8 and 2.0.1 utilizing CATHARE steam tables were used for chugging simulations of this study. In the OpenFOAM simulations, the version 1.7.1 of the code was used with incompressible formulation as it had already been used in a POOLEX (STB-31) case operating with lower DCC rates [24]. The compressible flow solver OpenFOAM 2.3.x was tested also. The transport equations for mass, momentum and energy are solved by NEPTUNE_CFD 1.0.8 for both continuous phases are [21]:

$$\frac{\partial}{\partial t}(\alpha_k \rho_k) + \nabla \cdot (\alpha_k \rho_k \mathbf{U}_k) = \Gamma_k \tag{1}$$

$$\frac{\partial}{\partial t}(\alpha_k \rho_k \mathbf{U}_k) + \nabla \cdot (\alpha_k \rho_k \mathbf{U}_k \mathbf{U}_k) = \alpha_k \nabla \cdot \left(\tau_{k,ij} + \tau^{t}_{k,ij}\right) - \alpha_k \nabla P + \alpha_k \rho_k \mathbf{g} + \mathbf{M}_k + \alpha_k \mathbf{S}_k \tag{2}$$

$$\frac{\partial}{\partial t}(\alpha_k \rho_k H_k) + \nabla \cdot (\alpha_k \rho_k \mathbf{U}_k H_k) = \alpha_k \frac{\partial P}{\partial t} + \alpha_k \rho_k \mathbf{U}_k \mathrm{g} - \nabla \cdot \left(\alpha_k \mathbf{Q}_k\right) + \Gamma_k H_k + \Pi_k + q'''_{\mathrm{wall},k}, \tag{3}$$

where Γ_k is the mass transfer rate, H_k is the total enthalpy, Π_k is the bulk interfacial heat transfer rate, $\mathbf{M}_k$ is the interfacial momentum transfer rate, and $\mathbf{S}_k$ is the external head loss term (which is not needed in this study). $\mathbf{M}_k$ term contains the momentum transfer by a drag model i.e. Large Interface Model of Coste 2013 [22] or the 'separated phase drag model' [21]. The Coste model takes also the interfacial tangential shear into account whereas the separated phase model applies the normal drag force only. Denoting liquid phase with $k = 1$ and vapor phase with $k = 2$, the mass transfer rate by phase change can be formulated as

$$\Gamma_k = \frac{\Pi_1 + \Pi_2}{H_2 - H_1}. \tag{4}$$

The vapor phase heat transfer contribution Π_2 is negligible compared to the liquid phase one in these simulations with saturated steam. Thus the interfacial heat transfer for liquid phase is defined only as

$$\Pi_1 = a_i h_1 (T_{sat} - T_1), \tag{5}$$

where a_i is the interfacial area density (m^{-1}), which is calculated from the gradient of void fraction (i.e., $a_i = |\nabla \alpha_1|$). The heat transfer coefficient for the water phase is defined as

$$h_1 = \frac{Nu_1 \lambda_1}{L_{t,1}}, \tag{6}$$

where λ is the thermal conductivity and L_t is the characteristic length. For the Nusselt number in chugging simulations, the correlations predicting high condensation rates in separated flow cases [22] have been promising [9]. In this study, the condensation models of Hughes and Duffey (HD) [14] and Coste (Coste C) [23] have been used;

$$Nu_1 = \frac{2}{\sqrt{\pi}} Re_{t,1} Pr^{1/2}, \text{ and} \tag{7}$$

$$Nu_1 = Re_{t,1}^{7/8} Pr^{1/2}, \tag{8}$$

respectively. The Reynolds number is defined as

$$Re_{t,1} = \frac{u_{t,1} L_{t,1}}{\nu_1}, \tag{9}$$

where the turbulent velocity $u_{t,1}$ is based on turbulence kinetic energy k_1 and dissipation rate ε_1. In the HD STB-28 simulations, $u_{t,1} = (\nu_1 \varepsilon_1)^{1/4}$ and in the HD DCC-05 simulations $u_{t,1} = \min(|\mathbf{U}_1|, C_\mu^{1/4} k^{1/2})$ are used. They produce negligibly different results. In the Coste C cases, $u_{t,1} = (2k_1/3)^{1/2}$ is used. The length scale in the HD and Coste C simulations are

$$L_{t,1} = C_\mu \frac{k_1^{3/2}}{\varepsilon_1}, \text{ and} \tag{10}$$

$$L_{t,1} = \left(\frac{\nu_1^3}{\varepsilon_1}\right)^{1/4}, \tag{11}$$

respectively. The standard k-ε model is used in the simulations with standard wall functions. The local k, ε values and the C_μ model constant (= 0.09) are obtained from the k-ε model.

The corresponding conservation equations of the OpenFOAM cases are presented in [24]. The heat transfer model in the OpenFOAM case is the same as the HD model in the NEPTUNE_CFD case in Eqs. (4) – (11).

3.2. Simulation models

3.2.1. Computational grids

It was observed in early simulation try-outs, that small cells at the pipe tip and abrupt changes of cell size tend to be major causes for convergence problems in the chugging cases. With the spherically curvilinear grid, the abrupt changes in grid cell sizes could be avoided and the amount of cells reduced. The grid used in the POOLEX STB-28 simulations (Fig. 8a) was an axisymmetric grid containing 12 716 hexahedral cells. A 3D grid was used in the simulations of the PPOOLEX DCC-05 case (Fig. 8b). The 3D version of the computational grid contained 0.8 million hexahedral cells. The POOLEX grid was refined inside the blowdown pipe to y+ ~ 5 and the PPOOLEX grid to y+ ~ 90 corresponding the inlet mass flow rates of steam. For the wall functions it was assumed y+ > 30, which is not an optimal value. However, this did not cause problems or visible errors in the NEPTUNE_CFD solution.

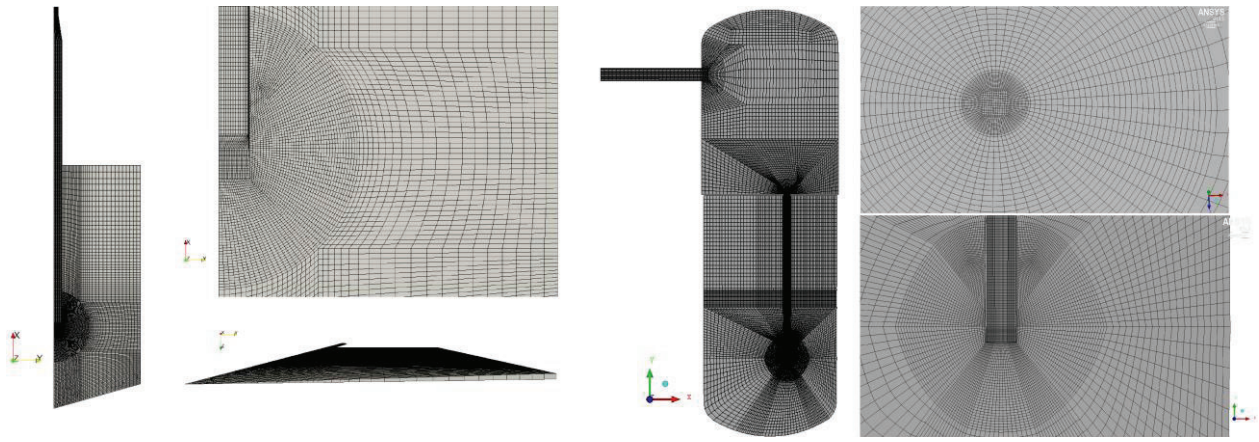

(a) (b)

Figure 8. 2D-axisymmetric grid (a) in the STB-28 simulations, and 3D grid (b) in the DCC-05 simulations.

For this paper, grid sensitivity studies have not yet been performed, but the preliminary tests indicate that qualitative interfacial behavior and obtained interfacial area can be changed more or less by the grid refinement, but the total condensation rate is not as sensitive to grid resolution in the end. However, it has to be noted that in Eulerian simulations without interfacial tracking the missing interfacial forces cannot be remedied completely by the grid refinement.

3.2.2. Simulation set-up

In all the simulations, the standard k-ε turbulence model was used for both of the phases. The NEPTUNE_CFD simulations were carried out with compressible flow solution utilizing the available steam tables of the CATHARE code. The first OpenFOAM simulation was done with an incompressible flow solver and the later with a compressible one with ideal gas assumption. The correlation of HD (Eq. 7) was used as the liquid phase heat transfer model in all the cases, although some DCC-05 cases were simulated by using Coste C (Eq. 8) correlation. Vapor phase heat transfer was omitted and saturated vapor was assumed. The cases presented in this paper are summarized in Table I and the main initial conditions in the DCC-05-4 simulations can be seen in Fig. 9 (a).

Table I. Simulated test samples

Alias	Test case	Code	Grid	DCC model	Interfacial mom. transfer
NE-S28-1	STB-28-1	NEPT 1.0.8	2D-axi, POOLEX	HD	Sep.ph
NE-S28-4	STB-28-4	NEPT 1.0.8	2D-axi, POOLEX	HD	Sep.ph
NE-S28-7	STB-28-7	NEPT 1.0.8	2D-axi, POOLEX	HD	Sep.ph
OF-I-S28-4	STB-28-4	OF 1.7.1	2D-axi, POOLEX	HD	Schiller-Naumann
OF-C-S28-4	STB-28-4	OF 2.3.x	2D-axi, POOLEX	HD	Schiller-Naumann
NE-D5-4-HDLI (a) (b) [1])	DCC-05-4	NEPT 2.0.1	3D PPOOLEX	HD	Coste LI
NE-D5-4-HDSE	DCC-05-4	NEPT 2.0.1	3D PPOOLEX	HD	Sep.ph
NE-D5-4-CO	DCC-05-4	NEPT 2.0.1	3D PPOOLEX	COSTE	Coste LI
NE-D5-4-HD-T	DCC-05-4	NEPT 2.0.1	3D PPOOLEX [2])	HD	Coste LI

[1]) (a) Initial steam interface at 0.7985 m, (b) at 1.8 m, [2]) Wetwell only
Abbreviations: NEPT –Neptune_CFD, OF – OpenFOAM, HD –Hughes-Duffey 1991,
COSTE – Coste 2004, Sep.ph – separated phase drag 'SIMMER'

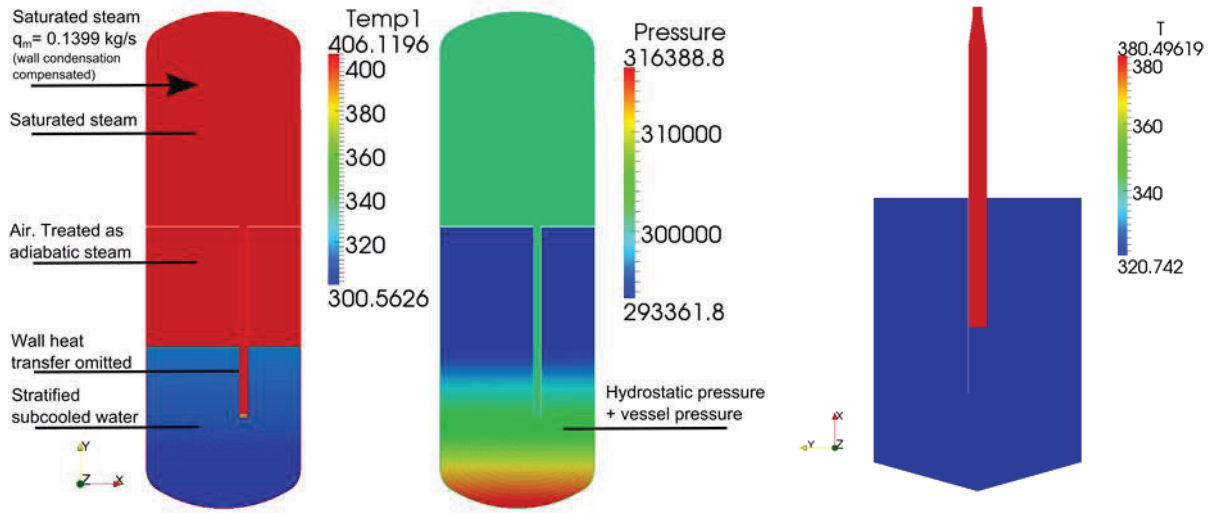

Figure 9. Initial fields in the simulations of (a) the DCC-05-4 test, and (b) the STB-28-1 test.

Although the wall condensation in the blowdown pipe is not simulated, it is taken into account by decreasing inlet mass flow rate both in the STB-28 and DCC-05 simulations. In the STB-28 simulations the pool water is initialized to uniform temperatures i.e. 321, 341, and 350 K for the STB-28-1, 4, and 7 cases respectively (Fig. 9 (b)). In the DCC-05 simulations stratified temperature fields were used.

4. RESULTS AND DISCUSSION

4.1. POOLEX STB-28 chugging cases

More comprehensive analysis and results of NE-S28-1, NE-S28-4, and NE-S28-7 simulations have been presented in [13]. The main finding from these simulations is the presence of quite realistic chugging. Fig. 10 includes samples of volume fraction fields from the NEPTUNE_CFD case NE-S28-4 and from the OpenFOAM cases OF-I-S28-4 and OF-C-S28-4.

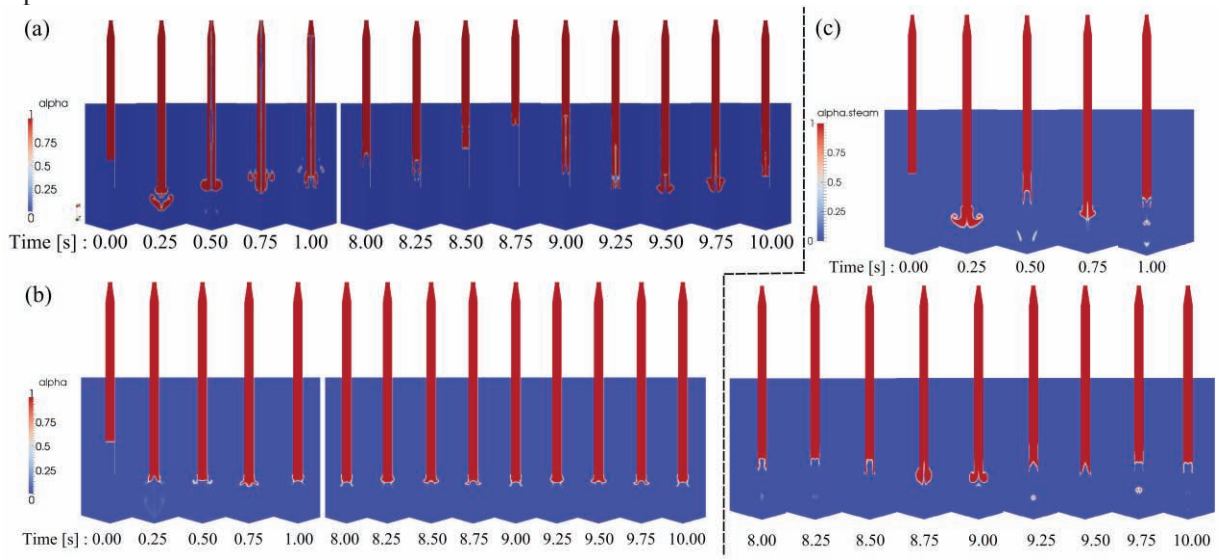

Figure 10. Volume fraction of steam in the 2D-axisymmetric NEPTUNE_CFD and OpenFOAM simulations of the STB-28-4 chugging test, (a) NE-S28-4, (b) OF-I-S28-4, (c) OF-C-S28-4.

Compressible flow formulation seems to be a requirement for chugging. Proper chugging was not observed in the incompressible case although all the steam was condensed in the vicinity of blowdown pipe outlet. Fig. 11 shows the DCC rate in the cases NE-S28-1, NE-S28-4, NE-S28-7, OF-I-S28-4, and OF-C-S28-4.

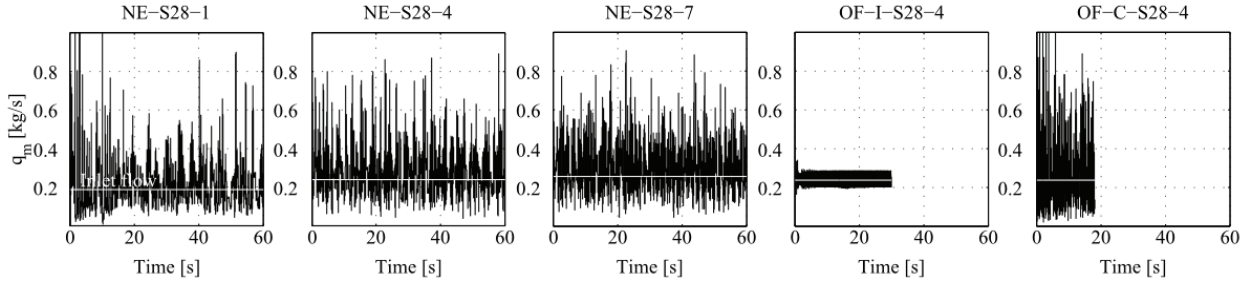

Figure 11. Condensation mass flow rates and inlet mass flow rate of steam in the 2D-axisymmetric NEPTUNE_CFD and OpenFOAM simulations of the STB-28 chugging test.

The main differences between the NEPTUNE_CFD and OpenFOAM simulations are the compressibility and the interfacial drag model. Differences in the interfacial (e.g. turbulence) modelling are also possible. Studies concerning the difference in the steam retreat depth (chugging frequency) between the compressible NEPTUNE_CFD and OpenFOAM solvers are underway.

In the NEPTUNE_CFD simulations of the STB-28 cases, chugging was qualitatively realistic enough for comparison with the pattern recognition results from the video data of the experiment. Fig. 12 presents the bubble width distributions in the NE-S28-1, NE-S28-4, and NE-S28-7 cases.

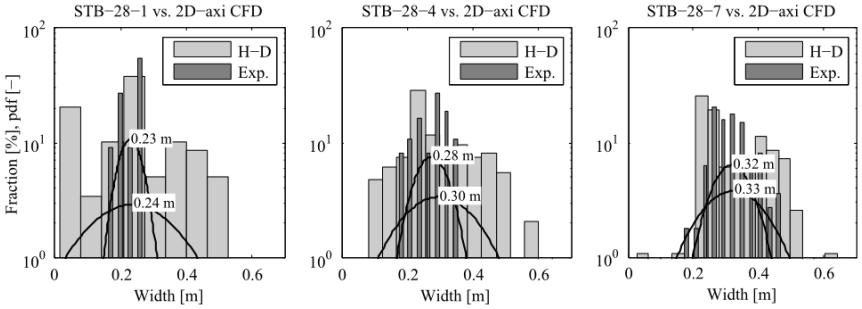

Figure 12. Bubble size distribution (maximum width of fully inflated ellipsoidal bubbles) in the 2D-axisymmetric NEPTUNE_CFD simulations of the STB-28 chugging test [13].

Although the uncertainties in the early pattern recognition models used in the STB-28 case are high [9, 13], the result is promising especially for the lower pool subcooling levels i.e. NE-S28-7 case. Fig. 13 shows the corresponding chugging frequencies obtained with the same pattern recognition model.

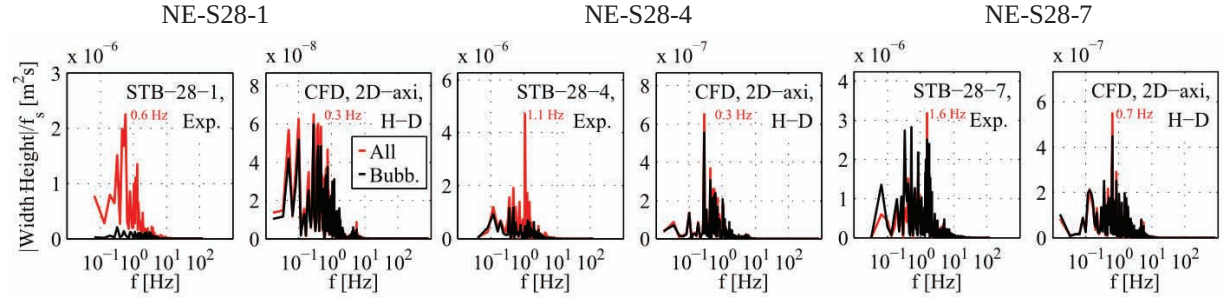

Figure 13. Power spectra of geometric mean of dimensions of bubbles and jets in the 2D-axisymmetric NEPTUNE_CFD simulations of the STB-28 chugging test [13].

The chugging frequencies at the exit of the blowdown pipe are qualitatively in the same range in the test and simulations. As the pool water heats up, larger and more numerous bubbles (instead of rapidly condensing jets) form at the mouth of the blowdown pipe due to decreasing condensation rate. It seems also that in the simulations more bubbles form instead of jets that form more frequently in the tests. The chugging frequencies are smaller in the simulations than in tests. Smaller frequencies in simulations indicate a higher condensation rate (i.e. chugging takes place inside the vent pipe). On the other hand, a larger fraction of fully inflated ellipsoidal/toroidal bubbles indicate slower than measured condensation rates in the calculations. To obtain more reliable results, 3D simulations and 3D imaging should be employed. More information concerning the cases NE-S28-1, NE-S28-4 and NE-S28-7 is available in [13].

4.2. PPOOLEX DCC-05 chugging cases

Although some promising 3D test simulations were done for the STB-28-4 case too [9], the better camera instrumentation of the PPOOLEX facility makes the later experiments more appealing for the DCC model validation purposes. The DCC rates in the NE-D5-4-HDLI and NE-D5-4-HDSE cases are presented in Fig. 14.

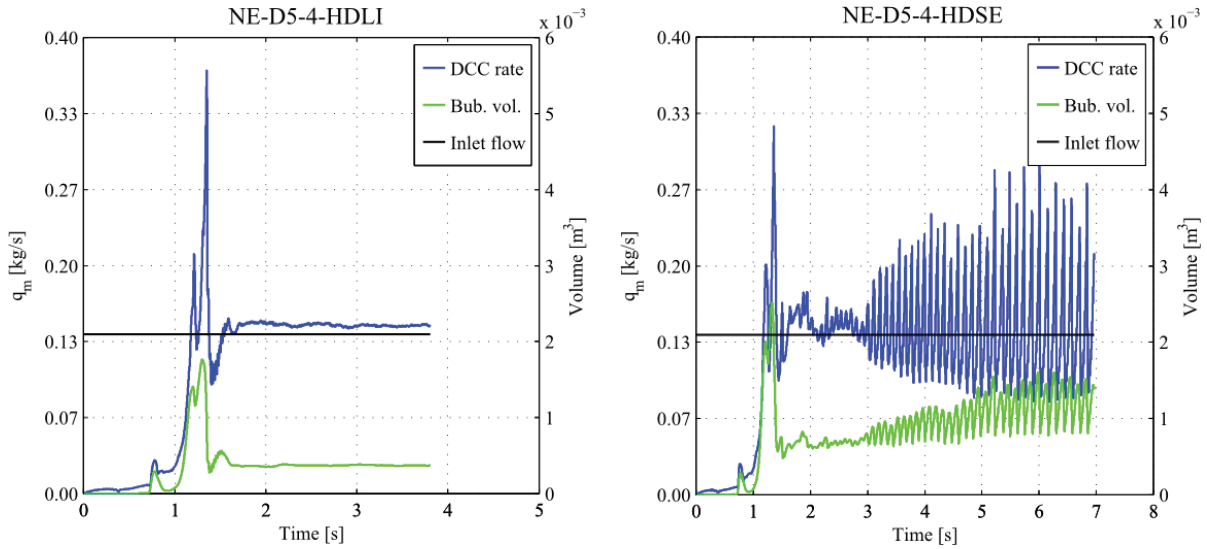

Figure 14. Condensation mass flow rates and bubble volume by Hughes & Duffey condensation model in the 3D NEPTUNE_CFD simulations of the DCC-05 chugging test.

Fig. 14 shows that the calculated condensation rate is high enough to suppress all the steam injected, but chugging is not reproduced as the bubble volume does not fall to zero in the NE-D5-4-HDLI and NE-D5-4-HDSE cases, there is continuously a bubble at the blowdown pipe outlet. Quite unphysically, the bubble does not oscillate in the NE-D5-4-HDLI case. The bubble oscillates if the drag model is the basic separated phase model (in NE-D5-4-HDSE). The DCC rate in the NE-D5-4-CO case is presented in Fig. 15.

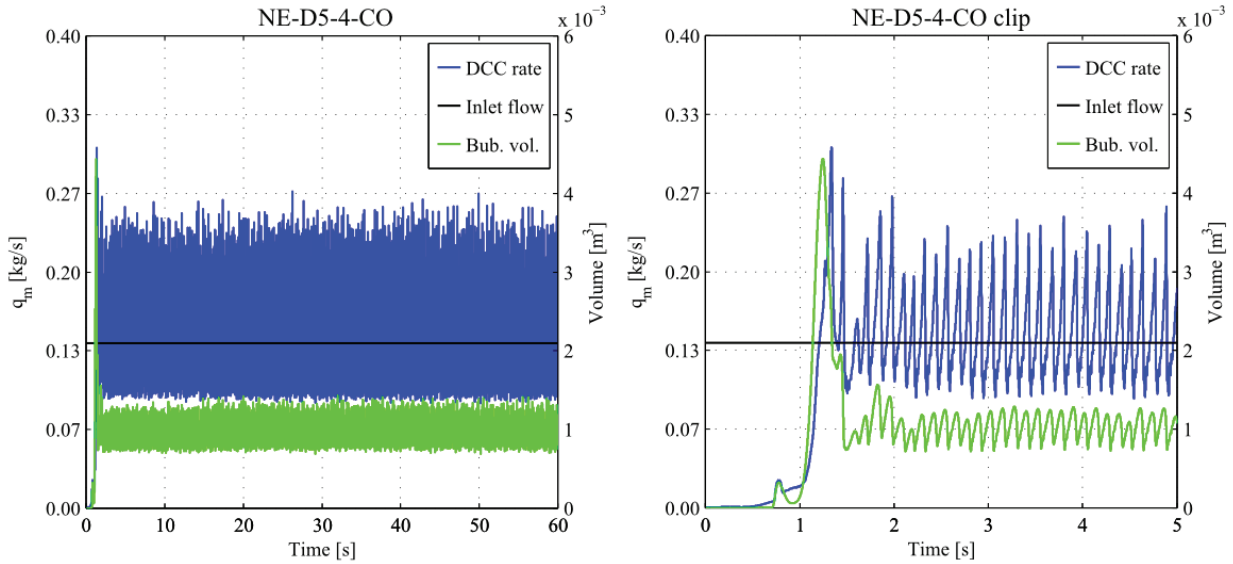

Figure 15. Condensation mass flow rates and bubble volume by Coste 2004 condensation model in the 3D NEPTUNE_CFD simulations of the DCC-05 chugging test.

Fig. 15 shows that the DCC rate and bubble volumes in the NE-D5-4-CO case are near the results of the NE-D5-4-HDSE case. The large interface drag model of Coste [22] gives now better results i.e. oscillating bubble, but the DCC rate is still too small to cause chugging. Weak DCC rate or missing chugging is not a new problem in the drywell-wetwell simulations, see e.g. [8]. Fig. 16 (a) presents the DCC rate for the case without the drywell in the geometry (NE-D5-4-HD-T).

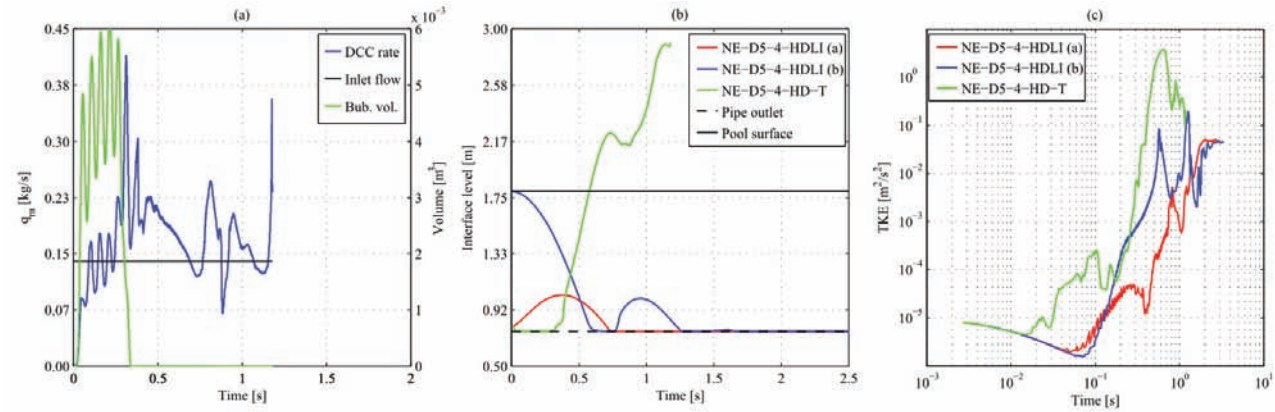

Figure 16. Condensation mass flow rates and bubble volume (NE-D5-4-HD-T case), internal chugging, and interfacial liquid turbulence kinetic energy level by Hughes & Duffey condensation model in the simulations of the DCC-05 chugging test. Effects of interface initialization and drywell.

If the drywell is bypassed in the calculations, the steam volume collapses into the blowdown pipe (Fig. 16 (b)) after the initial vigorously oscillating bubble (Fig. 16 (a) at 0 - 0.3 s). Within the blowdown pipe an internal chug occurs at 0.7 s. Turbulence kinetic energy grows much higher in the case without the drywell (Fig. 16 (c)), which in turn enhances condensation rate (Eqs. 9 - 10). Not even a higher initial interface elevation (NE-D5-4-HDLI (b)) lead to as good results. It seems that the drywell has a strong dampening effect on the chugging in the CFD simulations. Although the separated flow heat transfer models are promising in the cases without drywell, more accurate models are needed for DCC in a complete drywell-wetwell system. Particularly, the modelling of interfacial area under rapid condensation is an issue to be studied.

5. CONCLUSIONS

Suppression pool tests has been carried out at Lappeenranta University of Technology with the open-top wetwell facility POOLEX and with the drywell-wetwell suppression pool facility PPOOLEX. It has been demonstrated that the sizes and formation and break up rates of steam bubbles in the test video data can be measured by using a pattern recognition algorithm. Obtained bubble size data can then be compared with the field data from CFD simulations for the validation purposes of heat transfer models. The separated flow heat transfer model by Hughes and Duffey [14] has proven promising in the chugging simulations of the POOLEX STB-28 test. The compressible flow NEPTUNE_CFD simulations using that model reproduce the chugging behavior of the test qualitatively. However, the bubble size and chugging frequency spectra do not match that well between the simulations and the tests. The incompressible flow OpenFOAM simulation of the same case does not reproduce the chugging even qualitatively, although the condensation rate is high enough to condense the steam in vicinity of the blowdown pipe outlet. A compressible flow solver version produced chugging, but indicated smaller steam volume retreat depth in the blowdown pipe than was observed in NEPTUNE_CFD cases. The interfacial turbulence modelling and the ideal gas assumption in the OpenFOAM are likely reasons for the different results than with the NEPTUNE_CFD.

In the simulations of a drywell-wetwell system (the DCC-05 PPOOLEX experiment), the NEPTUNE_CFD simulations with a full geometry did not lead to strong chugging conditions observed in the experiment. All the condensation models tested in this study i.e. the Hughes and Duffey [14] and Coste [23] models failed to produce chugging. This differs negatively from the results of the open pool POOLEX chugging simulations. Despite of missing chugging, the condensation rates of the heat transfer models were high enough to condense the detaching steam bubbles in the vicinity of the blowdown pipe outlet.

In order to find the reason for the missing chugging, a higher initial location of the steam interface within the blowdown pipe was tested as well as the removal of the drywell from the geometry. The higher initial interface elevation did not cause chugging although it increased the interfacial turbulence level. The removal of the drywell led instead to initiation of chugging. Although the successfully simulated sample is short, it shows that the drywell functions as a damper in the simulations i.e. as an absorbing pressure boundary condition. Such an equilibrium restorative boundary makes the margin for the tolerable inaccuracies in the physical modelling very narrow. The heat transfer and interfacial area density models need to be developed further for more realistic simulation results in the drywell-wetwell suppression pool systems. Also, the computational grid size effects on the result should be studied further.

ACKNOWLEDGMENTS

The research leading to these results is partly funded by the European Atomic Energy Community's (Euratom) Seventh Framework Programme FP7/2007-2011 under grant agreements No. 232124 and No. 323263. The research is also funded partly by the Finnish Nuclear Waste Management Fund (VYR) via The Finnish Research Programmes on Nuclear Power Plant Safety SAFIR2010 and SAFIR2014.

REFERENCES

1. R. Lahey and F. Moody, *The Thermal-Hydraulics of a Boiling Water Reactor*, Chapter 11, American Nuclear Society, USA (1993).
2. I. Aya and H. Nariai, "Occurrence threshold of pressure oscillations induced by steam condensation in pool water," *Bulletin of JSME.* **29**(235), pp. 2131-2137 (1986).
3. S.M. Ali, V. Verma and A.K. Ghosh, "Analytical thermal hydraulic model for oscillatory condensation of steam in presence of air," *Nucl. Eng. and Des.*, **237**, pp. 2025-2039 (2007).
4. H. Li, W. Villanueva and P. Kudinov, *Effective Momentum and Heat Flux Models for Simulation of Stratifcation and Mixing in a Large Pool of Water,* NKS-266. NKS, ISBN 978-87-7893-339-3 (2012).

5. M. Meier, G. Yadigaroglu and M. Andreani, "Numerical and experimental study of large steam-air bubbles injected in a water pool," *Nucl. Sci. Eng*., **136**, pp. 363-375 (2000).
6. G. Yadigaroglu, "Computational Fluid Dynamics for nuclear applications: from CFD to multi-scale CMFD," *Nucl. Eng. Des.*, **235**, pp. 153-164 (2004).
7. R. Thiele, "Modeling of direct contact condensation with OpenFOAM," *Division of Nuclear Reactor Technology, Royal Institute of Technology, KTH*, Sweden. Master thesis, ISSN 0280-316X (2010).
8. T.J.H. Pättikangas, J. Niemi, J. Laine, M. Puustinen and H. Purhonen, "CFD modelling of condensation of vapour in the pressurized PPOOLEX facility," in: *CFD for Nuclear Reactor Safety Applications (CFD4NRS-3) Workshop*, Bethesda, MD, USA, 14-16 September 2010, p. 12. (2010)
9. V. Tanskanen, "CFD modelling of direct contact condensation in suppression pools by applying condensation models of separated flow," Ph.D. thesis, *Acta Universitatis Lappeenrantaensis 472.* Lappeenranta University of Technology. ISBN 978-952-265-221-8, ISBN 978-952-265-222-5 (2012).
10. S.Q. Li, P. Wang and T. Lu, "Numerical simulation of direct contact condensation of subsonic steam injected in a water pool using VOF method and LES turbulence model," *Prog. Nucl. Energy*, **78**, pp. 201-215 (2015).
11. S.S. Gulawani, S.K. Dahikar, C.S. Mathpati, J.B. Joshi, M.S. Shah, C.S. RamaPrasad and D.S. Shukla, "Analysis of flow pattern and heat transfer in direct contact condensation. *Chem. Eng. Sci.,* **64**, pp. 1719-1738 (2009).
12. H.S. Kang and C.H. Song, "CFD analysis for thermal mixing in a subcooled water tank under a high steam mass flux discharge condition," *Nucl. Eng. and Des*., **238**, pp. 492-501 (2008).
13. V. Tanskanen, A. Jordan, M. Puustinen and R. Kyrki-Rajamäki, "CFD simulation and pattern recognition analysis of the chugging condensation regime," *Annals of Nucl. Energy*, **66**, pp. 133-143 (2014).
14. E.D. Hughes and R.B. Duffey, "Direct contact condensation and momentum transfer in turbulent separated flows," *Int. J. of Multiphase Flow*, **17**, pp. 599-619 (1991).
15. M. Puustinen, R. Kyrki-Rajamäki, V. Tanskanen, A. Räsänen, H. Purhonen, V. Riikonen, J. Laine and E. Hujala, "BWR suppression pool studies with POOLEX and PPOOLEX test facilities at LUT," in: *The 15th International Topical Meeting on Nuclear Thermal Hydraulics (NURETH-15)*, Pisa, Italy, May 12-17 2013, pp. 1-12 (2013).
16. J. Tuunanen, J. Kouhia, H. Purhonen, V. Riikonen, M. Puustinen, R. S. Semken, H. Partanen, I, Saure and H. Pylkkö, "General description of the PACTEL test facility," *VTT Research Notes 1929*, VTT, Finland, ISBN 951-38-5338-1 (1998).
17. S. Chen, F. Gerner and C. Tien, "General film condensation correlations," *Exp. Heat Transfer*, **1**, pp. 93-107 (1987).
18. S. Ghiaasiaan, *Two-Phase Flow, Boiling, and Condensation in Conventional and Miniature Systems*, 1st edition, Cambridge University Press, New York, ISBN 978-0-521-88276-7 (2008).
19. D. Bestion and A. Guelfi, "Status and perspective of two phase flow modelling in the NEPTUNE multiscale thermalhydraulic platform for nuclear reactor simulation," *Nucl. Eng. and Tech.*, **37**(6), pp. 511-524 (2005).
20. A. Guelfi, D. Bestion, M. Boucker, P. Boudier, P. Fillion, M. Grandotto, J.M. Hérard, E. Hervieu and P. Péturaud, "NEPTUNE: A new software platform for advanced nuclear thermal hydraulics," *Nucl. Sci. and Eng*., **156**, pp. 281-324 (2007).
21. J. Laviéville, E. Quémérais, S. Mimouni, M. Boucker and N. Méchitoua, "NEPTUNE CFD V1.0 theory manual," *Technical Report. EDF* (2006).
22. P. Coste, "A Large Interface Model for two-phase CFD," *Nucl. Eng. and Des.*, **255**, pp. 38-50 (2013).
23. P. Coste, "Computational Simulation of Multi-D Liquid-Vapor Thermal Shock with Condensation," *Proceedings of ICMF'04*, Yokohama, Japan, May 30 - June 4 (2004).
24. G. Patel, V. Tanskanen and R. Kyrki-Rajamäki, "Numerical modelling of low-Reynolds number direct contact condensation in a suppression pool test facility," *Annals of Nucl. Energy*, **71**, pp. 376-387 (2014).